1964

The effects of granular size on the thermal conductivity of fine sand

Fikri Yalvac

Department:

THE EFFECTS OF GRANULAR SIZE
ON THE
THERMAL CONDUCTIVITY OF FINE SAND

BY

FIKRI YALVAC, 1933

A

THESIS

Submitted to the faculty of the

UNIVERSITY OF MISSOURI AT ROLLA

in partial fulfillment of the requirements for the

Degree of

MASTER OF SCIENCE, MECHANICAL ENGINEERING

Rolla, Missouri

1964

Approved by

(Adviser)

ABSTRACT

The Thomas method (1) for determining the thermal conductivity of solid materials can be used for the determination of the thermal conductivity of granular materials. In this thesis this method has been used to determine the effect of the granular size of sand on its thermal conductivity.

River sand was classified according to size by the Tyler Standard Screen Scale into 50 − 60, 60 − 80, 80 − 100, 100 − 200, and below 200 mesh size. These sands were used for the experiments. The clay was separated from these samples to obtain pure river sand for the experiments.

According to the International Critical Tables, the thermal conductivity of sand, k, is between 0.1728 and 0.2212 Btu/hr-ft-°F in the range of 32 - 320°F. In the experiments performed, a temperature range of 80 - 150°F was used, and the results obtained were close to the reported values. The effective thermal conductivity increased for the first three samples of 50 − 60, 60 − 80, 80 − 100 mesh size of the Tyler Standard Screen Scale, but it decreased for the last samples of the very fine granular sand, 100 − 200, and below 200 mesh size.

The experiments were performed under atmospheric pressure without convective currents.

The purpose of these experiments was to determine the

effect of the granular size of sand on the thermal conductivity. The results obtained regarding very small grain size were of particular interest.

The results are expressed in Table 7 and Graph 8.

ACKNOWLEDGEMENTS

The author would like to acknowledge the assistance of Dr. A. J. Miles, his major adviser, and of Dr. Harry J. Sauer, Jr. in the preparation of this thesis. He would like to express his appreciation to the members of the staff of the Mechanical Engineering Department Laboratory.

TABLE OF CONTENTS

LIST OF ILLUSTRATIONS

LIST OF TABLES

LIST OF GRAPHS

NOMENCLATURE

c	Specific heat, Btu/lb_m-°F.
D_p	Average diameter of packing material, ft.
h_{rs}	Heat transfer coefficient for radiation, solid to solid, Btu/hr-ft^2-°F.
h_{rv}	Heat transfer coefficient for radiation, void to void, Btu/hr-ft^2-°F.
K	Thermal diffusivity, ft^2/hr.
k	Thermal conductivity, Btu/hr-ft-°F.
k_{e^o}	Effective thermal conductivity of packed bed, Btu/hr-ft-°F.
k_g	Thermal conductivity of fluid, Btu/hr-ft-°F.
k_s	Thermal conductivity of packing material, Btu/hr-ft-°F.
q	Heat flux per unit area, Btu/hr-ft^2.
r	The polar coordinate radius, ft.
R	The inside radius of the inner tube, ft.
T	Temperature, °F.
T_c	Temperature at the center of specimen, °F.
T_s	Temperature at the surface of specimen, °F.
t	Time, hr.
w	Heat capacity, Btu/ft^2-°F.
θ	Fraction void.
β	Ratio of the average length between the centers of two neighboring solids in the direction of heat flow to the mean diameter of particles.

γ Length of solid affected by thermal conductivity per mean diameter of solid.

φ Effective thickness of solid film in void in relation to thermal conduction per mean diameter of solid.

ϵ Emmissivity of solid surface.

I. INTRODUCTION

The object of this thesis is to determine the effects of the granular size on the thermal conductivity of fine sand.

Many scientists and engineers have been interested and worked on the thermal conductivity of packed granular materials for the last sixty years. None has reached any accurate mathematical formulation of concepts because of the unknown effects on the effective thermal conductivity of packed beds. Experimental research has shown that the analytical studies of several authors were not entirely satisfactory. (Additional experiments were conducted here on sand with smaller grain size than in previous experiments by other investigators.) Before any conclusions can be reached, it is necessary to know the physical properties and the environmental conditions of the packed materials. Among these properties are grain size, grain uniformity, grain shape, material and its thermal properties, porosity, etc. In addition it is necessary to know the fluid in the pore space, its physical and thermal properties, and permeability of the packed granular material. It was observed from the experiment that the results obtained on humid days were slightly different than the others. Hence, it is very necessary that the experiment be conducted without presence of moisture and under uniform environment. Decreasing the porosity by compressing the granulae has a large effect on the effective thermal

conductivity. The experiments in this thesis were performed in low moisture content weather in the Mechanical Engineering Laboratory, and the packing was prepared by shaking the apparatus with horizontal hand strokes on the side of the tube. Uniform conditions of weather and packing were maintained during the experiment and data taking.

The granular material used was river sand graded and classified as to fineness by a Tyler Screen Scale into five sizes. The last two, or smaller, sizes of sand samples were washed and screened to remove any trace of clay and silt that may have been present.

Yagi and Kunii's (3) equations were used as an analytical approach for the purpose of comparison and better understanding for the theory involved.

II. LITERATURE SURVEY

Engineers and scientists have been interested in the thermal conductivity of many materials. In some instances a high thermal conductivity is desirable and values as high as 260 Btu/hr-ft-°F, in the case of metals, are of interest. For the purpose of insulation, values of thermal conductivity of 0.025 Btu/hr-ft-°F, in the case of cork, are desirable. Both composite and purest materials are of interest, although they give some difficulty in determining their thermal conductivity. Perhaps this is due to variations in pore size and shape, and permeability, and to the nature of the contacts between grains or particles.

A. EXPERIMENTAL METHOD

The determination of the thermal conductivity of the material is generally conducted using the following methods: (1) a steady state temperature distribution (2) a constantly rising temperature on a constant temperature gradient resulting from a constant heat input. The second method was used in this thesis.

In the Vernotta method for determining the conductivity a constant heat flux through a uniform slab can be produced. From the temperatures at each face and the quantity of heat flow the thermal conductivity can be determined. There is, however, a physical difficulty in preventing heat flux at the edges of the slab.

Yagi and Kunii (3) used an experimental method which involves a long duration of time and a large mass of material

for the measurement of effective thermal conductivity in packed beds with motionless air. The granular material was packed in a cylindrical device, and heat applied to the surface by means of electric resistance heaters. After about three to six hours, the temperature rose at a uniform rate at all radii. Knowing the temperature, the rate of temperature rise, weight of the materials, specific heat, and heat input, the thermal conductivity was determined.

In the Thomas method (1), thermal conductivity of granular materials is determined by measuring the temperature changes at the center and surface of a metal cylinder containing the material. Heat is supplied to the cylinder wall at a constant rate by a resistance winding, and surface heat loss is eliminated by an outer screening tube kept at the same temperature as the container of the granular material by manual or automatic control. The material is placed in the thin walled metal cylinder of the apparatus on which there is a resistance winding R_1. The wall is heated at a constant rate by the current in the winding (resistance R_1, Figure 1). The temperature measurements are made by three thermocouples; one at the center of the inner cylinder, one attached to the inner surface of the inner cylinder, and the other attached to the inner surface of the outer cylinder. Taking into account the heat capacity of the wall, the mathematical theory shows that when the surface heat flux is uniform the temperature difference between the center and the surface finally becomes a constant, and the rate of rise of temperature is the same everywhere within the cylinder; that is, at all radii.

Heat from the cylinder winding (resistance R_1) is dissipated both by conduction into the interior and by convection, conduction, and radiation to its external surroundings. If the heat loss is eliminated due to the external surroundings, the heat flux through the material can be determined. In order to eliminate the heat loss due to the external surroundings, the temperature of the inner face of the outer tube is kept at the same temperature as the surface of the inner tube by manual control of the resistance R_2 over the outer tube, Figure 1.

Eliminating the external heat losses, and supplying the inner tube with constant and known heat flux, the temperatures at the wall of the inner cylinder, and at the center are recorded against time. As a result the two curves, the wall temperature, and the central temperature of the inner tube versus time, are almost linear and parallel to each other. The reason for this is the small change of thermal conductivity of the specimen (sand) with temperature which can be assumed as a constant. This helps in simplifying the mathematical solutions.

The temperature distribution along the vertical axis in the tube is practically uniform but,as can be seen from experimental results, there is no perfect uniformity. The temperature in the middle is slightly less than the temperatures near the ends.

If long tubes are used, these effects become smaller. In these experiments it is better to record the middle temperatures because it is more likely that there is one dimensional heat transfer at the middle than at the ends of the tube. $\partial T/\partial x \approx 0$ at the middle, and therefore there is one dimensional heat transfer there.

By choosing the right points to record the temperatures, and proving by experiments that the temperature distribution along the vertical axis is very close to uniformity. It can be assumed there is one dimensional heat transfer. The formula according to Fourier can be set up for the case of symmetrical radial heat flow; the differential equation is:

$$\partial^2 T/\partial r^2 + (1/r)\,(\partial T/\partial r) = (1/K)\,(\partial T/\partial t) \quad . \quad . \quad . \quad . \quad (1)$$

where:

T : the temperature, °F

r : the polar coordinate radius, ft.

K = k/cρ

k : the thermal conductivity, Btu/hr-ft-°F

c : the specific heat, Btu/lb_m-°F

ρ : the density, lb_m/ft^3

t : the time, hr.

When r = R

$$q = K\,(\partial T/\partial r) + w\,(\partial T/\partial t) \quad . \quad . \quad . \quad . \quad . \quad . \quad . \quad . \quad . \quad . \quad (2)$$

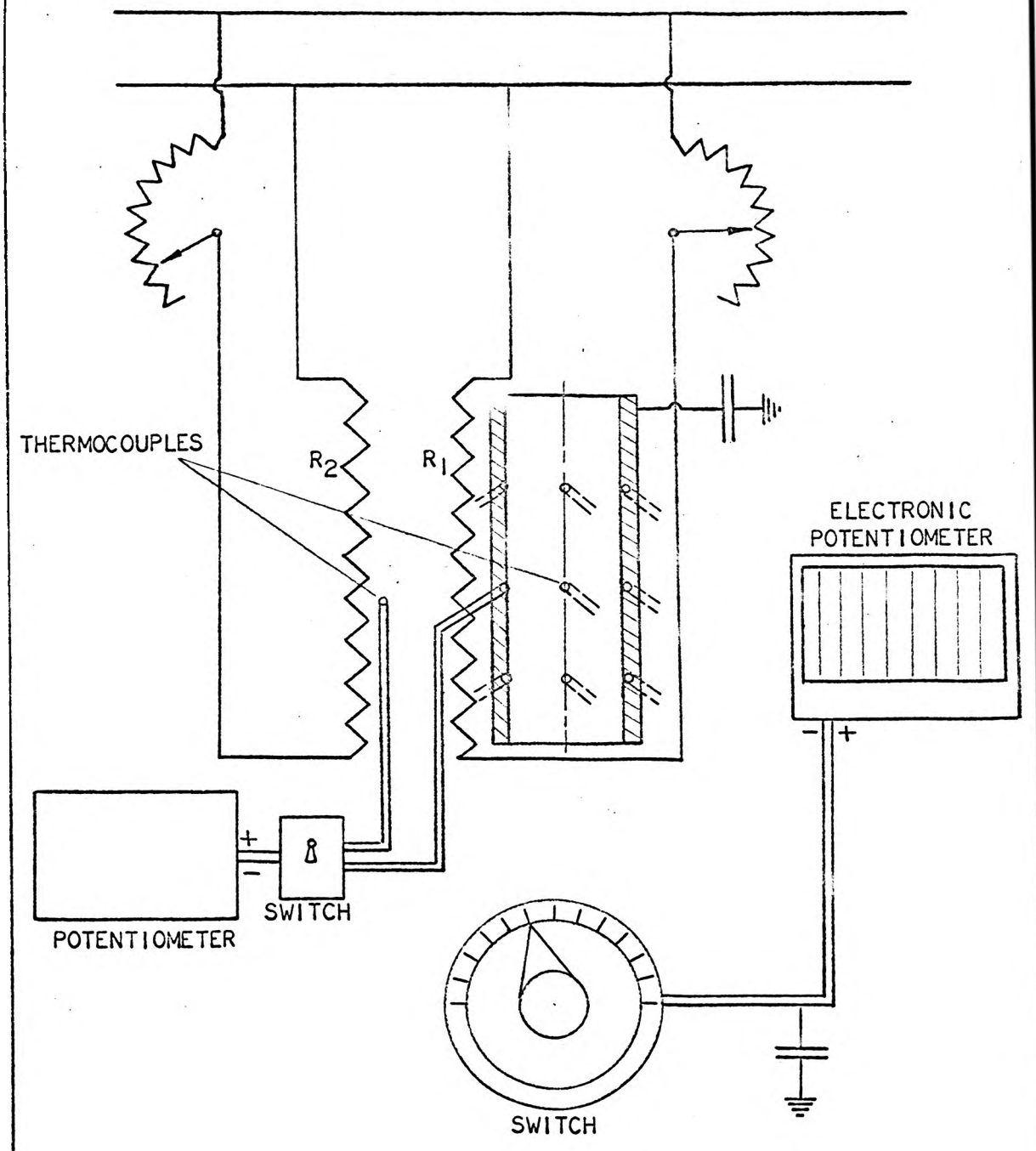

FIGURE 1. SCHEMATIC DESCRIPTION OF THE APPARATUS

where:

q : the heat flux, Btu/ft^2-hr.

w : the heat capacity per unit area of the cylinder wall, Btu/ft^2-°F

Since the tube walls are thin and good heat conductors, the temperature difference between the faces of the wall is small, and for these reasons, the effects of the tube can be neglected. The solution of equation (1) is given in the appendix of this thesis. It was determined by Thomas (1) to be:

$$T = \frac{q}{w + (kR)/(2K)} \left[t + \frac{r^2}{4K} - \frac{R^2}{8K} \left(\frac{4Kw + kR}{2Kw + kR} \right) \right] . \quad . \quad . \quad . \quad (3)$$

$T = T_s$ when $r = R$

$$T_s = \frac{q}{w + (kR)/(2K)} \left[t + \frac{R^2}{4K} - \frac{R^2}{8K} \left(\frac{4Kw + kR}{2Kw + kR} \right) \right]$$

$T = T_c$ when $r = 0$

$$T_c = \frac{q}{w + (kR)/(2K)} \left[t - \frac{R^2}{8K} \left(\frac{4Kw + kR}{2Kw + kR} \right) \right]$$

$$T_s - T_c = (R^2 q)/2(2Kw + kR) \quad . \quad . \quad . \quad . \quad . \quad . \quad . \quad . \quad . \quad . \quad . \quad (4)$$

$$(\partial T/\partial t) = (2Kq) / (2Kw + kR) \quad . \quad . \quad . \quad . \quad . \quad . \quad . \quad . \quad . \quad (5)$$

Using (4) and (5);

$$K = [R^2 (\partial T / \partial t)]/4 (T_s - T_c) \quad . \quad . \quad . \quad . \quad . \quad . \quad . \quad . \quad . \quad (6)$$

Using (4) and (6);

$$k = R[q - w (\partial T/ \partial t)]/2 (T_s - T_c), \text{ Btu/hr-ft}^\circ\text{F}. \quad . \quad . \quad . \quad (7)$$

This gives the value of thermal conductivity, k, as desired.

$(\partial T/\partial t)$ is the slope of the time-temperature curve in $^\circ$F/hr.

B. ANALYTICAL METHOD

Granular materials are frequently the basis of heat insulation materials. No entirely satisfactory theoretical basis has yet been found for the advance prediction of the thermal conductivity of a granular material of known composition. Many attempts have been made for different cases and materials.

If the heat transfer across the air spaces in a granulated material was by conduction alone, the effective conductivity would be independent of the linear size of the grains for geometrically similar grain structures. "The effective conductivity would not be proportional to the conductivity of the grain material unless the ratio of the conductivity of the air to that of the grains were constant" (4). The points of contact of the grains are of immeasurable dimensions, whereas, in most granulated materials, the surfaces of contact are extremely small and the intervening air plays a very important part in the conduction of heat through the system.

Yagi and Kunii (3) found that there are seven processes in the heat transfer in granulated materials. The processes are:

Heat transfer mechanism independent of fluid flow

1. Thermal conduction through a solid,
2. Thermal conduction through the contact surfaces

of two particles,

3. Radiant heat transfer between the surfaces of two particles,

4. Radiant heat transfer between neighboring voids,

Heat transfer mechanism dependent on fluid flow

5. Thermal conduction through the fluid film near the contact surfaces of two particles,

6. Heat transfer by convection, solid-fluid-solid,

7. Heat transfer by lateral mixing of fluid, Figure 2.

In the case of the two dimensional model shown in Figure 3, mechanism 5 is calculated theoretically, and nearly all of the heat flows through the thin film near the contact points or surface of the two solids. Therefore the effect of the fluid flow by mechanism 5 is small because the fine interstices near the contact surfaces are embedded in the boundary layers except in the case of large Reynolds number. Mechanisms 1, 3, 4, and 5 are predominant when the Reynolds number is small because the boundary layers around the particles are thick compared with the distance between grains. Mechanism 7 controls the heat flow when the Reynolds number is large, therefore, mechanism 6 only slightly affects the total rate of heat flow. The theoretical heat transfer equations show that the effects of convectional heat transfer mechanism solid-fluid-solid are small at all Reynolds numbers; therefore the authors assume (3):

I. Thermal conduction through the thin film of fluid near the contact surfaces is not affected by fluid flow,

II. The convectional heat transfer mechanism solid-

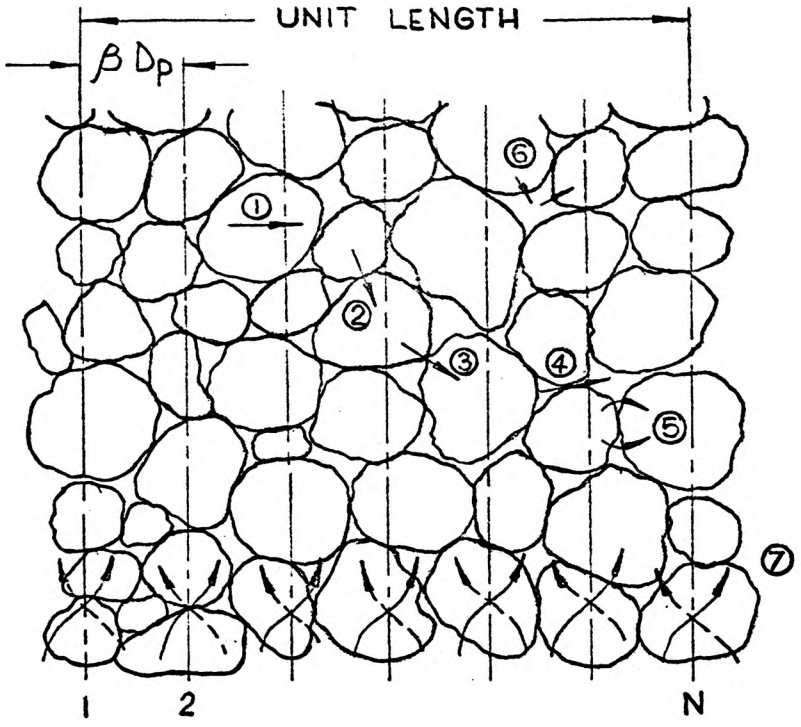

Figure 2, A model of heat transfer in packed beds showing the mechanisms, (2).

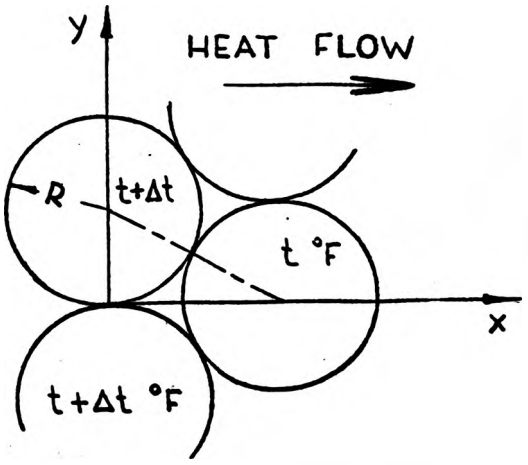

Figure 3, Two dimensional model of heat transfer through the fluid film in the void of the packed bed.

fluid-solid is less important than the other mechanisms and can be safely neglected.

From Yagi and Kunii's (3) descriptions of the heat transfer mechanisms in packed beds without flowing fluid, as shown in Figure 4 and 5, the heat transfer mechanism in the series having the thermal conduction in the solid phase arise in the fraction $(1 - \theta)$ of the sectional area C - C' therefore the radiant heat is transferred from one void to another through the fraction θ of the sectional area.

The heat transfer coefficient of thermal radiation is found by the equations (8a), (8b), (9a) and (9b). It is assumed the two voids A and B are respectively represented by the two parallel surfaces of black body A' and B' near the section C - C' as shown in Figure 4.

The coefficients from solid surface to solid surface

$$h_{rs} = 0.1952 \frac{\epsilon}{2 - \epsilon} \left[\frac{t + 273}{100} \right]^3 , \text{ kcal/hr-m}^2\text{-°C} \quad . \quad . \quad . \quad . \quad (8a)$$

$$h_{rs} = 0.04 \frac{\epsilon}{2 - \epsilon} \left[\frac{5t + 2297}{900} \right]^3 , \text{ Btu/hr-ft - F.} \quad . \quad . \quad . \quad . \quad (8b)$$

from void to void

$$h_{rv} = \frac{0.1952}{1 + \frac{\theta}{2(1-\theta)} \frac{1 - \epsilon}{\epsilon}} \left[\frac{t + 273}{100} \right]^3 , \text{ kcal/hr-m}^2\text{-c}_C \quad (9a)$$

$$h_{rv} = \frac{0.04}{1 + \frac{\theta}{2(1 - \theta)} \frac{1 - \epsilon}{\epsilon}} \left[\frac{5t + 2297}{900} \right]^3 , \text{ Btu/hr-ft}^2\text{-°F} \quad (9b)$$

Where:

h_{rs}: heat transfer coefficient for radiation solid to solid

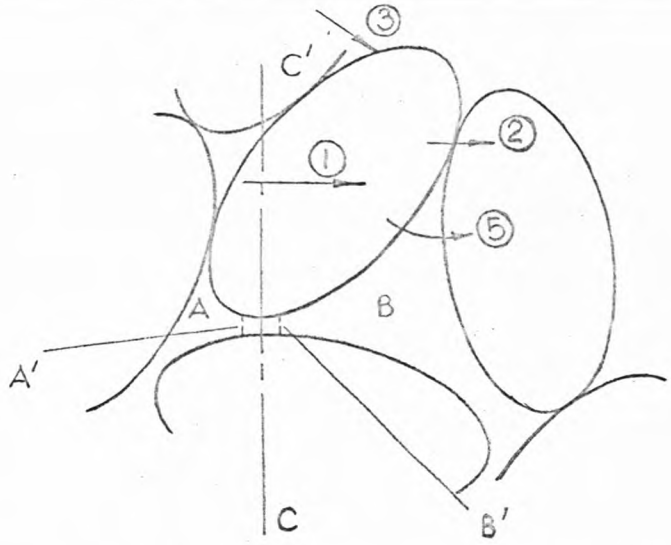

Figure 4, A model of heat transfer without flowing fluid.

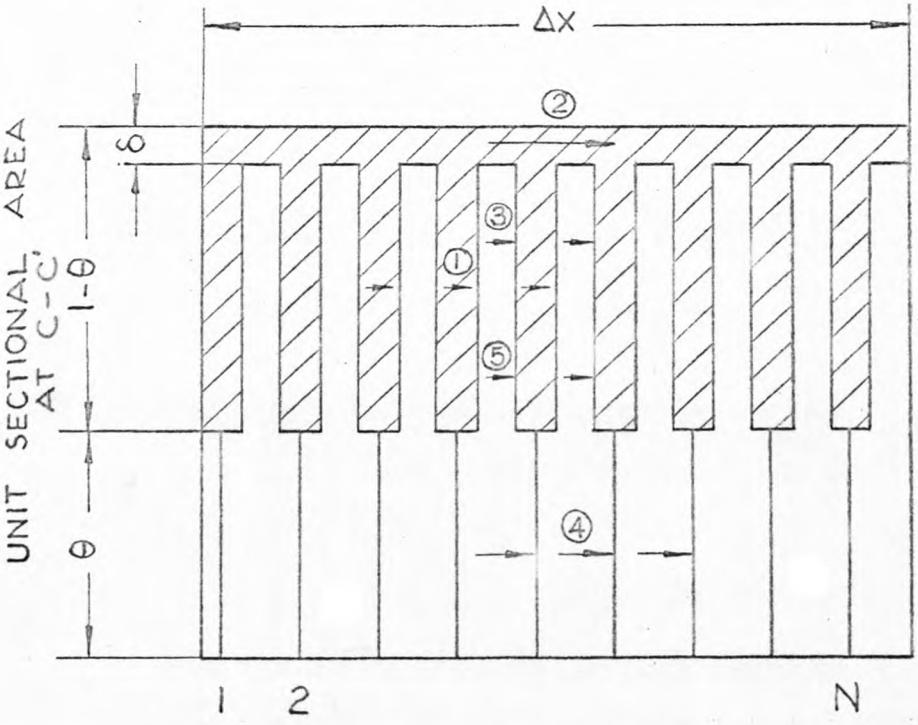

Figure 5, Simplified model of heat transfer in the packed bed without flowing fluid.

h_{rv}: heat transfer coefficient for radiation, void to void

ϵ : the emissivity of the solid surface

θ : the fraction void

Then the over-all heat transfer rate q is formulated as equation (10) by application of a model of heat transfer in a packed bed with motionless fluid as shown in Figure 5.

$$q = \frac{k_{e^o}}{\Delta x}\Delta t = \delta\frac{k_s}{\Delta x}\Delta t + U_s(1-\theta-\delta)\Delta t + U_v\theta\Delta t \quad (10)$$

$$\frac{1}{U_s} = N\Delta x\left(\frac{\ell_s}{k_s} + \frac{1}{\frac{k_g}{\ell_v} + h_{rs}}\right), \quad (11a)$$

$$\frac{1}{U_s} = N\Delta x\,\frac{\gamma D_p}{k_s} + \left(\frac{1}{\frac{k_g}{\varphi D_p} + h_{rs}}\right) \quad (11)$$

$$\frac{1}{U_v} = (N\Delta x)\,(1/h_{rv}) \quad (12)$$

Where:

$\gamma = \ell_s/D_p$, length of solid affected by thermal conductivity/mean diameter of solid. It is practically unity.

δ : total area of perfect contact surfaces as solid phase in sectional area of section C - C'/sectional area of section C - C'.

$\varphi = \ell_v/D_p$, effective thickness of fluid film in the void in relation to thermal conduction/ mean diameter of solid, Graph 1.

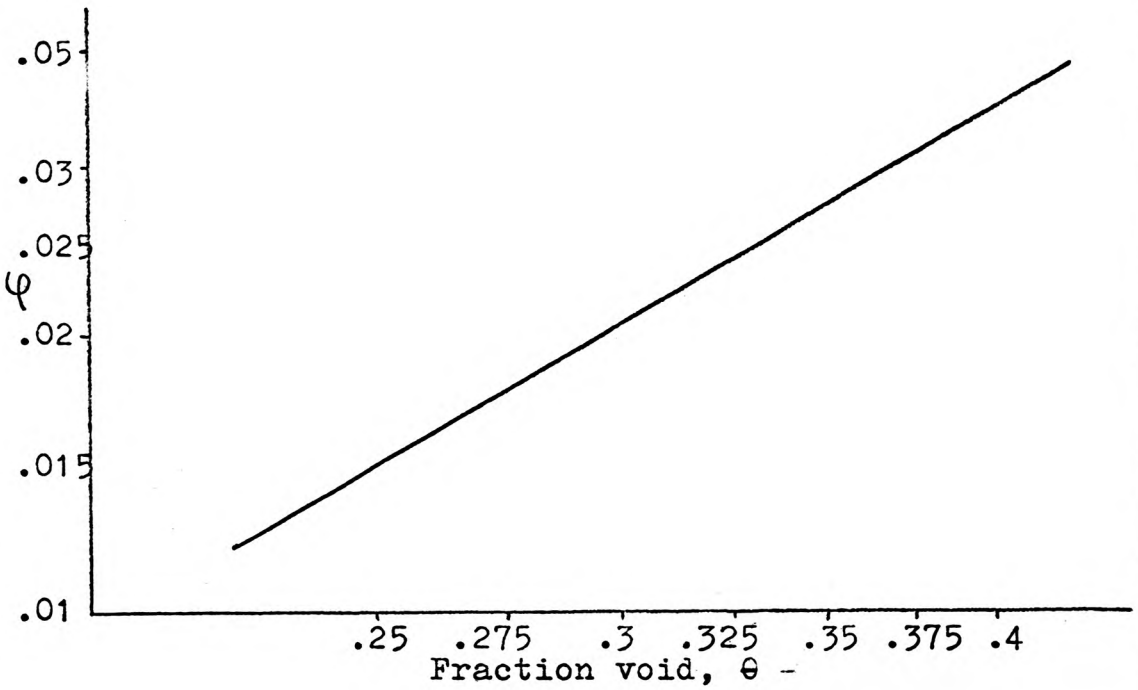

Graph 1, φ vs θ curve (3).

U_s : over-all heat transfer coefficient from solid surface to solid surface.

U_v : over-all heat transfer coefficient from void to void

ℓ_s : effective length of solid relating to thermal conduction.

ℓ_v : effective thickness of fluid film adjacent to contact surface of two solid particles.

$N = 1/\ell_p$, number of solids in the unit length of packed bed, measured in the direction of heat flow.

ℓ_p : effective length between the centers of grains.

k_{e^o} : effective thermal conductivity of the packed bed with motionless fluid.

k_s : thermal conductivity of the packing material.

k_g : thermal conductivity of the fluid.

From equations (10), (11), and (12), the equations for different cases are:

General equation

$$\frac{k_{e^o}}{k_g} = \frac{k_s}{k_g} + \frac{(1-\theta-\delta)}{\gamma\left(\frac{k_g}{k_s}\right) + \frac{1}{\frac{1}{\varphi} + \frac{D_p h_{rs}}{k_g}}} + (\theta\beta D_p h_{rv})/k_g \qquad (13)$$

In the case of gas-filled voids

$$\frac{k_{e^o}}{k_g} = \frac{\beta(1-\theta)}{\gamma\left(\frac{k_g}{k_s}\right) + \frac{1}{\frac{1}{\varphi} + \frac{D_p h_{rs}}{k_g}}} + \theta\beta\frac{D_p h_{rv}}{k_g} \quad \ldots\ldots\ldots \quad (14)$$

In the case of vacuum only

$$\frac{k_{e^o}}{k_g} = \delta + \frac{\beta(1-\theta)}{1 + \frac{k_s}{D_p h_{rs}}} \quad \ldots\ldots\ldots\ldots\ldots\ldots \quad (15)$$

In the case of fine particles with motionless gas filled voids

$$\frac{k_{e^o}}{k_g} = \beta(1-\theta)/\left(\frac{k_g}{k_s} + \varphi\right) \quad \ldots\ldots\ldots\ldots\ldots \quad (16)$$

$\beta = \frac{\ell_p}{D_p}$, for practical purposes β can be assumed as approximately unity.

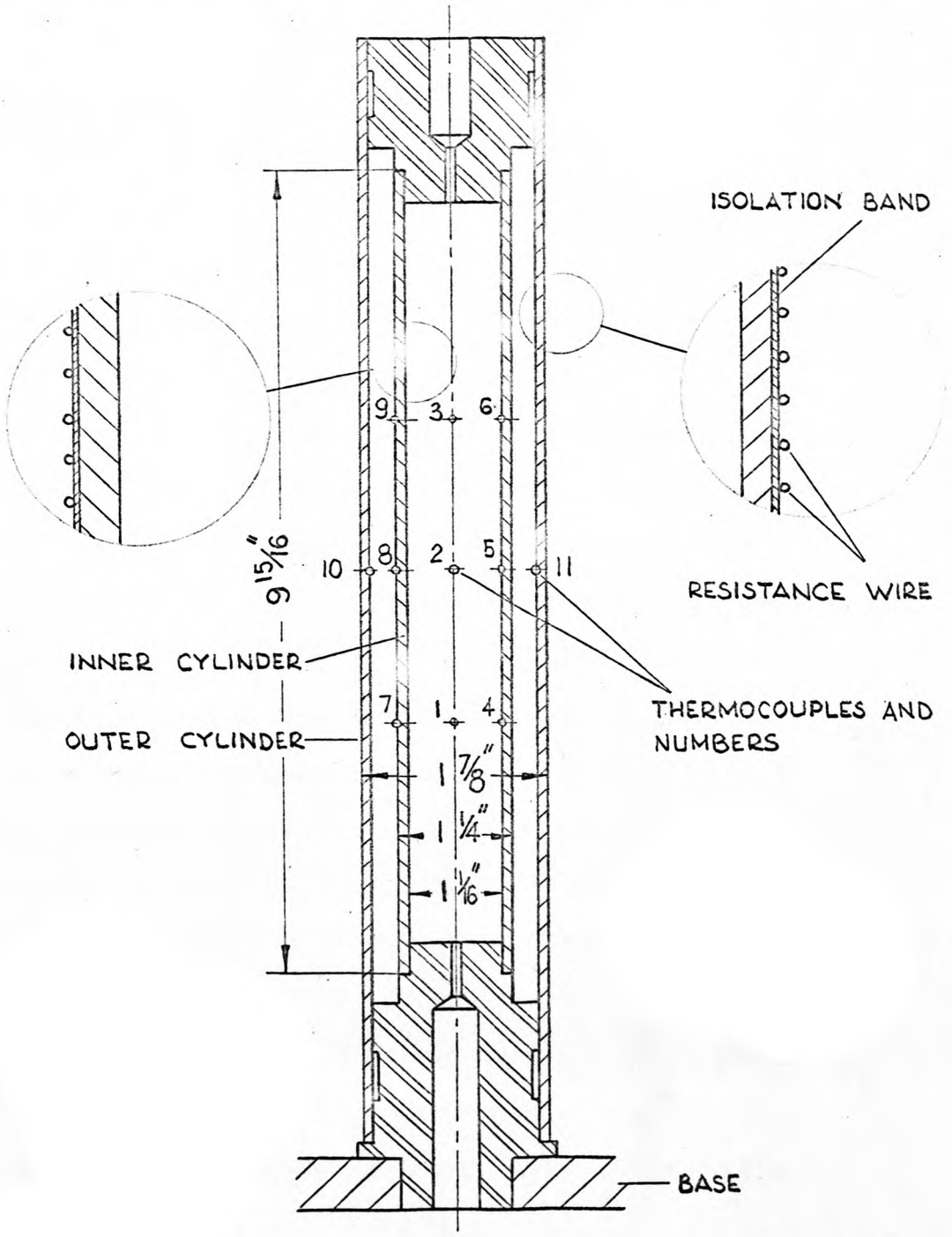

Figure 6, The apparatus for determining the thermal conductivity of granular materials.

III. APPARATUS

As can be seen from Figure 6, an inner aluminum tube 1-1/16 inches diameter, 9-15/16 inches long, and 3/32 inch wall thickness was used. The outer aluminum tube is 1-7/8 inches in diameter, and 13 inches long. Two wooden blocks were used to hold the tubes concentric and close the ends. Nichrome resistance wire was wound on both tubes with 10 turns per inch after isolating the surface of the tubes with a plastic band from the wire. Eleven thermocouples were installed as shown in Figures 1 and 6. The apparatus was mounted on a wooden base.

The two heaters supplied alternating current, and the input was controlled by two variable auto-transformers.

An electronic recording potentiometer was used to record the temperature distribution. In order to eliminate the effect of the induction due to the windings on the readings, two 2 mfd capacitors were used between the positive lead of the thermocouples and the ground; and between the inner tube wall and the ground, Figure 1. Another ordinary potentiometer was used to control the input of the heater to the outer tube. Thus a temperature equilibrium between the inner and outer tube surfaces could be obtained.

IV. EXPERIMENTS

After adjusting the input power of the inner tube heater, and choosing a less humid day, the inner tube was filled with the material to be tested. The temperatures at the center, and at the inner surface of the inner tube were measured by the electronic recording potentiometer. The temperatures at the inner surfaces of the inner and outer tubes were measured by the ordinary potentiometer. The initial temperature was set as the zero reading on the electronic recording potentiometer. Then both of the auto-transformers and the recording paper band of the electronic recording potentiometer were switched on to start the operation. The temperatures of the inner walls of the inner and outer tubes were read, and to maintain the temperature equilibrium between the two, the electric power supply to the outer tube through the heater was manually adjusted. At the same time the switch box was manually changed every 45 seconds between the central thermocouple and the one attached to the inner surface of the inner tube, Figure 1. A single experiment usually took thirty-six minutes. The data obtained was tabulated, and the temperature distribution was plotted. A copy of one of the recorded papers is submitted with each copy of this thesis.

Temperature Distribution Control Along the Vertical Axis

For this experiment the electronic recording potentiometer was used, and the temperatures at different points parallel to the vertical axis were recorded. There was no measurable temperature difference between the two sets of points, so the assumption concerning single dimensional heat transfer in the apparatus is proved, Graph 7.

TABLE 1

Data for sand

Sample No.	1	2	3	4	5
Sand size between Tyler Standard Screen Scale Mesh	50-60	60-80	80-100	100-200	Below 200
Sand size between sieve openings in inches	from 0.0098 to 0.0116	from 0.0070 to 0.0098	from 0.0059 to 0.0070	from 0.0029 to 0.0059	from 0.0005 to 0.0029
Average diameter of sand particles D_p, in inches	0.0107	0.0084	0.0065	0.0044	0.0017
Porosity, θ	0.379	0.371	0.358	0.392	0.352
* φ	0.032	0.0305	0.029	0.033	0.028

* φ taken from Graph 1

TABLE 2

Sample No. 1

Data for the plot of temperature as a function of time

Time in Minutes	Temp. T_c in °F	Temp. T_s in °F	Time in Minutes	Temp. T_c in °F	Temp. T_s in °F
0	76.4	76.4	20	108.7	115.8
1	76.4	79.4	21	110.5	117.6
2	76.9	81.9	22	112.3	119.4
3	77.9	83.9	23	114.2	121.2
4	79.3	85.9	24	116.0	123.0
5	81.0	87.9	25	117.7	124.7
6	82.9	89.9	26	119.5	126.5
7	84.7	91.9	27	121.3	128.3
8	86.6	93.9	28	123.1	130.1
9	88.5	95.9	29	124.8	131.9
10	90.4	97.7	30	126.6	133.6
11	92.3	99.5	31	128.4	135.4
12	94.0	101.3	32	130.3	137.3
13	95.9	103.2	33	132.1	139.1
14	97.8	105.1	34	133.9	140.8
15	99.7	106.9	35	135.7	142.6
16	101.5	108.6	36	137.4	144.4
17	103.3	110.4	37	139.3	146.2
18	105.1	112.2			
19	106.9	114.0			

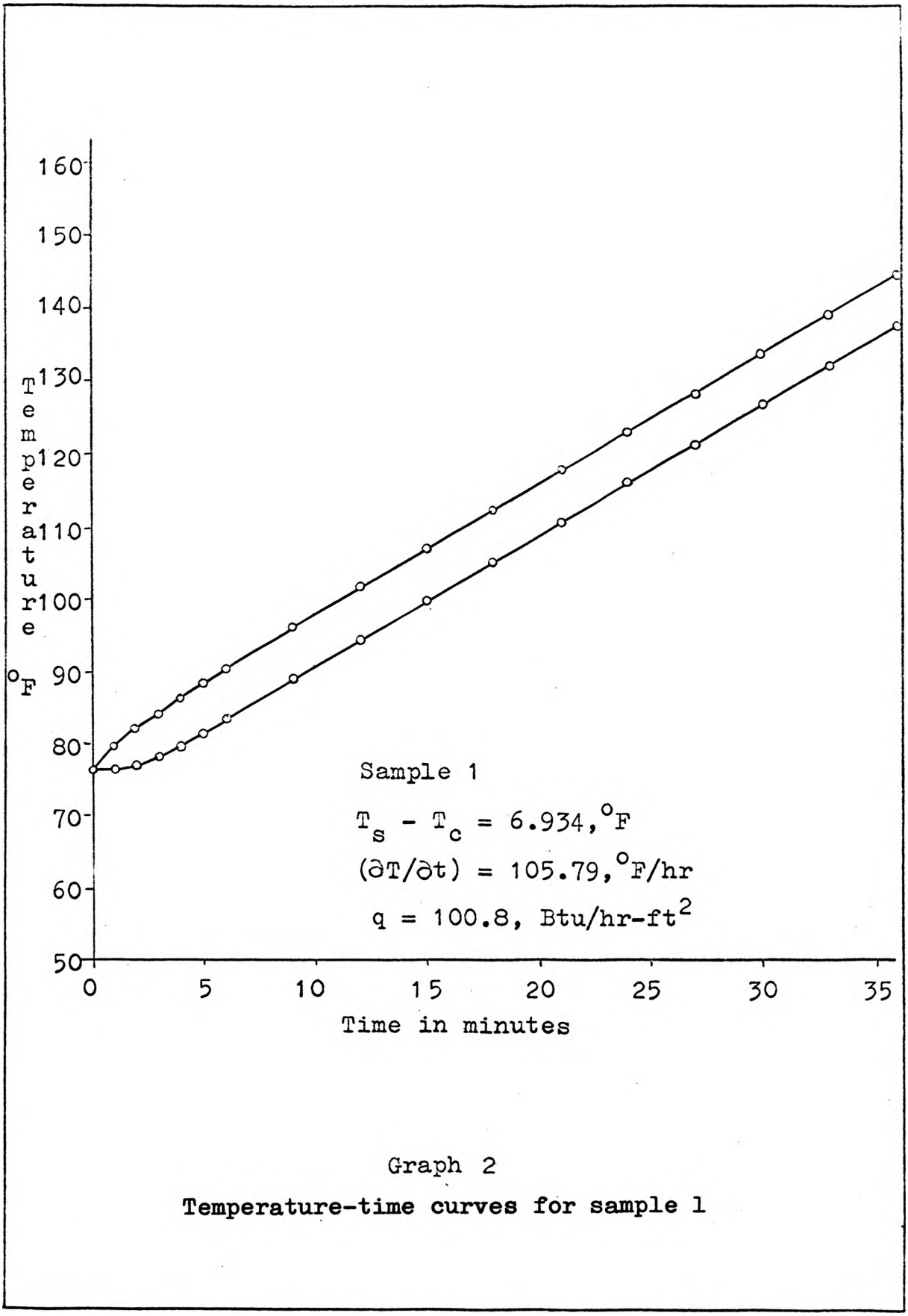

Graph 2

Temperature-time curves for sample 1

TABLE 3

Sample No. 2

Data for the plot of temperature as a function of time

Time in Minutes	Temp. T_c in °F	Temp. T_s in °F	Time in Minutes	Temp. T_c in °F	Temp. T_s in °F
0	76.4	76.4	20	109.7	116.4
1	76.4	79.4	21	111.6	118.2
2	77.2	81.8	22	113.5	120.2
3	78.4	83.9	23	115.4	121.9
4	79.9	85.9	24	117.2	123.6
5	81.5	88.0	25	118.9	125.4
6	83.4	89.9	26	120.6	127.2
7	85.2	91.9	27	122.4	129.0
8	87.1	93.9	28	124.3	130.8
9	89.1	95.9	29	126.1	132.5
10	91.0	97.8	30	127.9	134.3
11	92.9	99.6	31	129.6	135.9
12	94.8	101.4	32	131.4	137.9
13	96.8	103.4	33	133.4	139.8
14	98.6	105.3	34	135.3	141.6
15	100.4	107.1	35	137.0	143.4
16	102.2	108.9	36	138.8	145.2
17	104.0	110.7	37	140.5	146.9
18	106.0	112.6			
19	107.9	114.4			

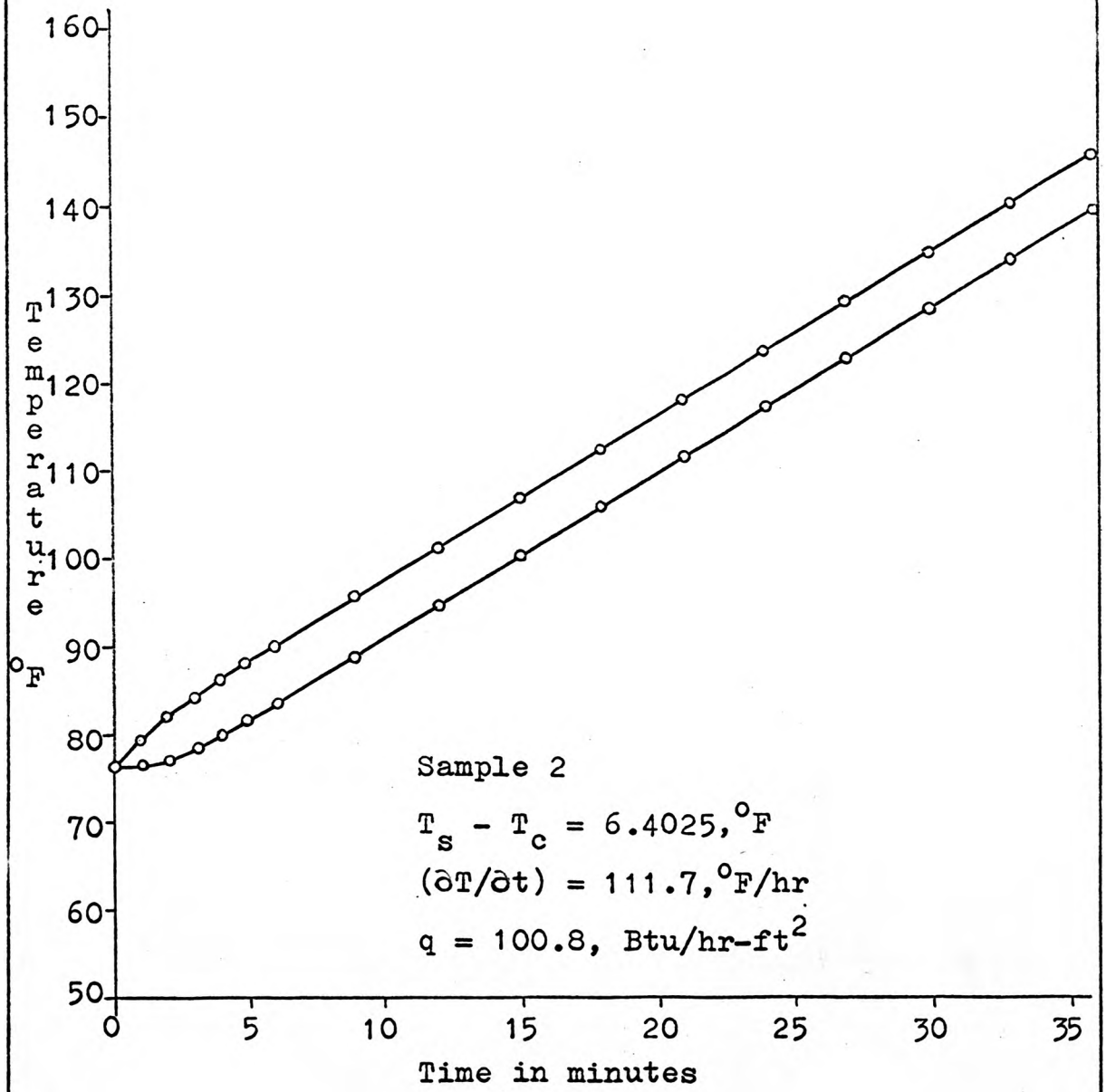

Graph 3

Temperature-time curves for sample 2

TABLE 4

Sample No. 3

Data for the plot of temperature as a function of time

Time in Minutes	Temp. T_c in °F	Temp. T_s in °F	Time in Minutes	Temp. T_c in °F	Temp. T_s in °F
0	78.4	78.2	20	111.8	118.0
1	78.4	81.2	21	113.6	119.8
2	79.2	83.4	22	115.4	121.6
3	80.4	85.7	23	117.2	123.4
4	82.0	87.7	24	119.1	125.3
5	83.7	89.7	25	121.0	127.1
6	85.4	91.7	26	122.8	128.9
7	87.2	93.6	27	124.6	130.7
8	89.2	95.5	28	126.4	132.5
9	91.2	97.4	29	128.2	134.3
10	93.2	99.4	30	130.1	136.1
11	95.1	101.4	31	131.9	138.0
12	96.9	103.2	32	133.7	139.8
13	98.8	105.2	33	135.5	141.6
14	100.7	107.1	34	137.3	143.3
15	102.6	108.9	35	139.0	145.0
16	104.4	110.7	36	140.7	146.8
17	106.2	112.5	37	142.4	148.5
18	108.1	114.3			
19	110.0	116.2			

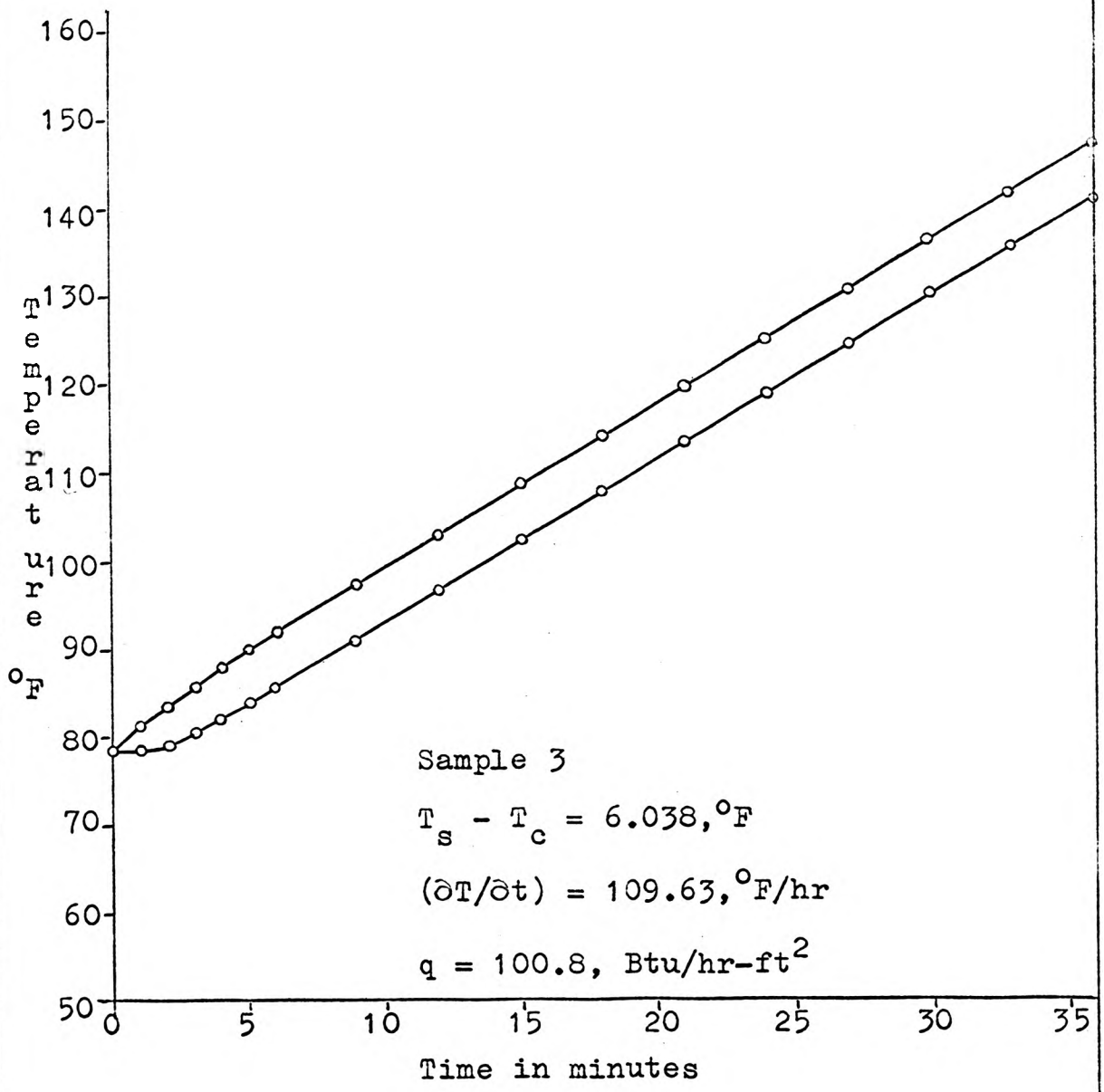

Graph 4

Temperature-time curves for sample 3

TABLE 5

Sample No. 4

Data for the plot of temperature as a function of time

Time in Minutes	Temp. T_c in °F	Temp. T_s in °F	Time in Minutes	Temp. T_c in °F	Temp. T_s in °F
0	76.6	76.6	20	109.8	117.0
1	76.6	79.7	21	111.7	118.8
2	77.2	82.2	22	113.6	120.7
3	78.5	84.5	23	115.5	122.6
4	79.9	86.6	24	117.3	124.5
5	81.6	88.6	25	119.1	126.3
6	83.4	90.5	26	120.8	128.0
7	85.1	92.5	27	122.6	129.7
8	87.1	94.4	28	124.5	131.6
9	89.0	96.4	29	126.3	133.4
10	90.9	98.3	30	128.1	135.2
11	92.7	100.1	31	129.9	136.9
12	94.6	102.0	32	131.6	138.6
13	96.6	103.9	33	133.5	140.5
14	98.5	105.8	34	135.3	142.2
15	100.5	107.7	35	137.0	144.0
16	102.4	109.6	36	138.8	145.7
17	104.2	111.5			
18	106.1	113.4			
19	108.0	115.2			

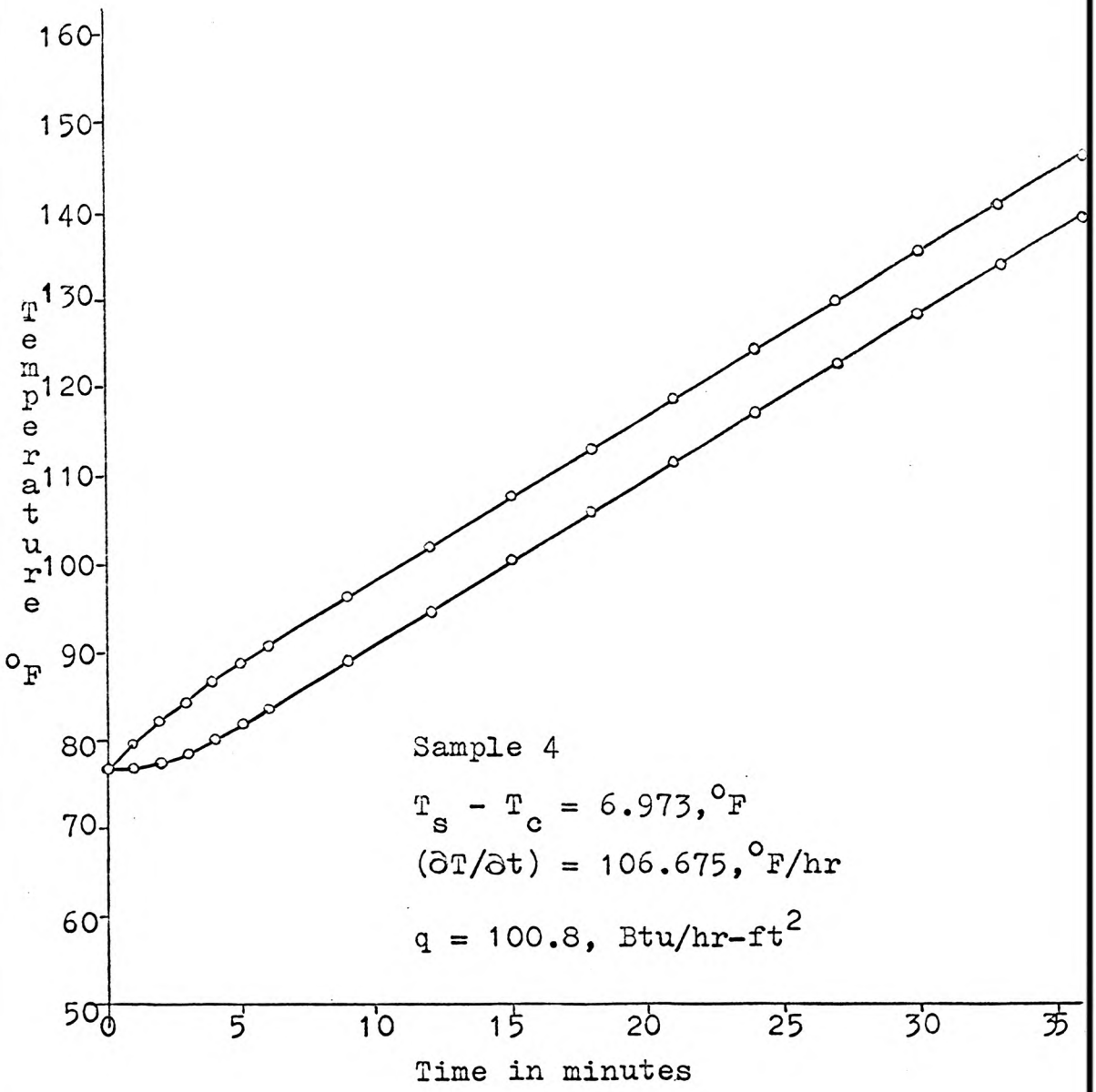

Graph 5
Temperature-time curves for sample 4

TABLE 6

Sample No. 5

Data for the plot of temperature as a function of time

Time in Minutes	Temp. T_c in °F	Temp. T_s in °F	Time in °F	Temp. T_c in °F	Temp. T_s in °F
0	70.7	70.7	20	104.5	111.5
1	70.7	74.0	21	106.5	113.4
2	71.5	76.5	22	108.6	115.6
3	73.0	78.8	23	110.5	117.5
4	74.3	80.8	24	112.5	119.4
5	76.0	82.8	25	114.5	121.5
6	77.8	84.7	26	116.6	123.4
7	79.7	86.7	27	118.7	125.5
8	81.5	88.6	28	120.6	127.4
9	83.4	90.4	29	122.5	129.4
10	85.2	92.2	30	124.2	131.0
11	87.0	93.9	31	126.0	132.8
12	88.9	96.0	32	127.8	134.7
13	90.8	97.8	33	129.7	136.6
14	92.6	99.6	34	131.6	138.5
15	94.6	101.6	35	133.6	140.4
16	96.6	103.5	36	135.6	142.3
17	98.6	105.5	37	137.4	144.2
18	100.5	107.5			
19	102.6	109.5			

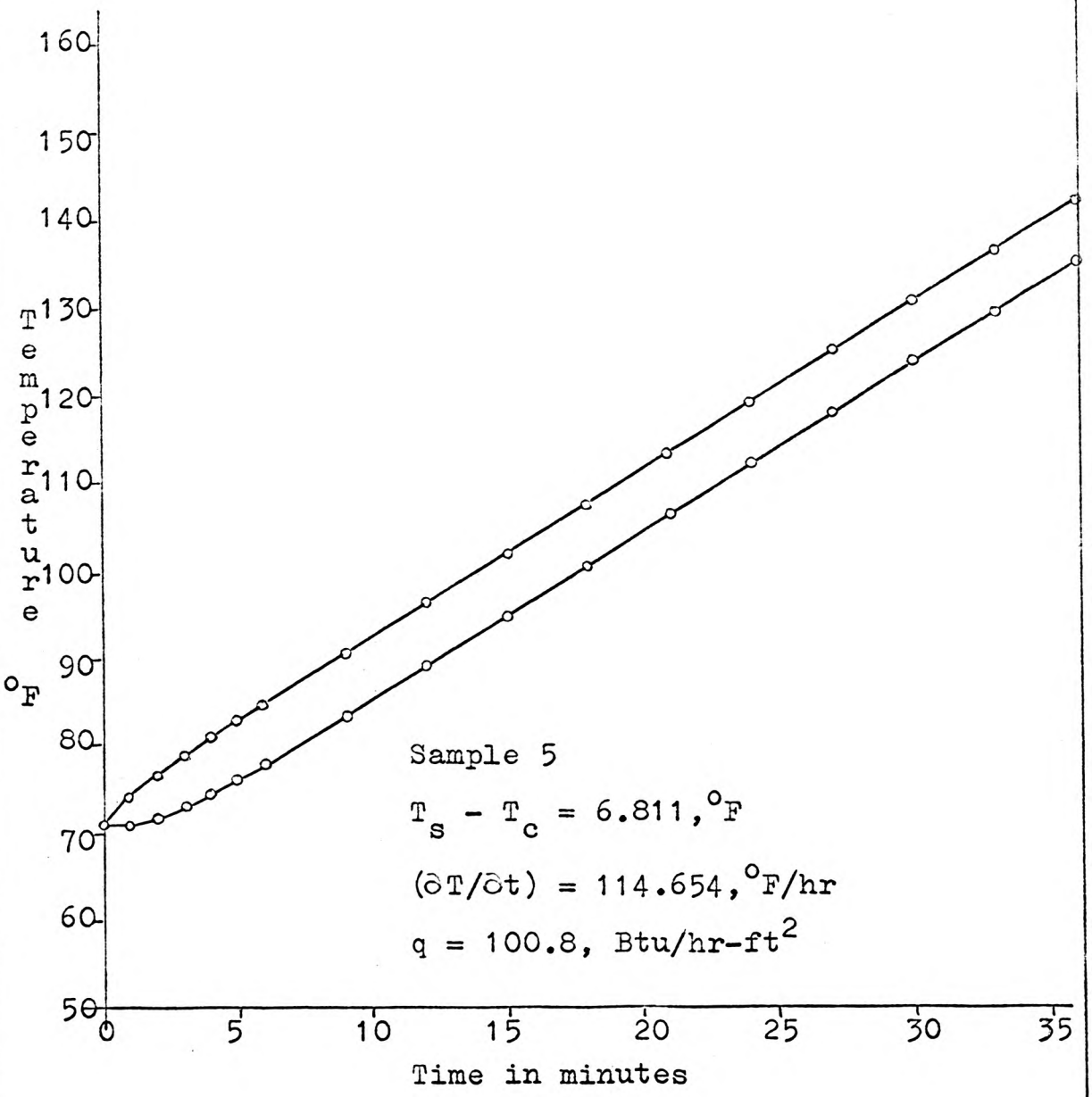

Graph 6

Temperature-time curves for sample 5

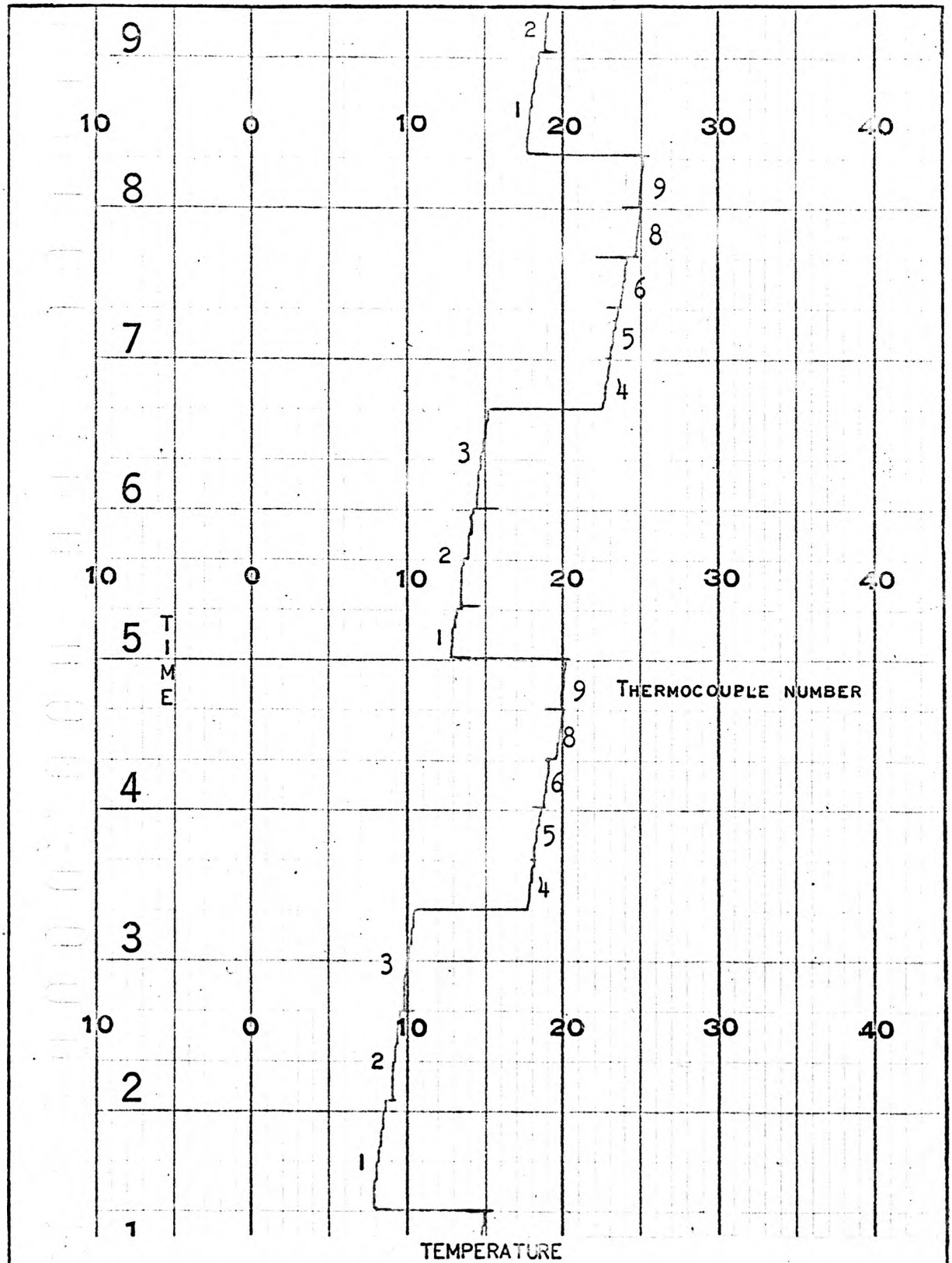

GRAPH 7. THE ORIGINAL GRAPH OF THE ELECTRONIC POTENTIOMETER TO SHOW THE TEMPERATURE DISTRIBUTION ALONG THE AXIS.

V. CALCULATIONS

1. Calculations for the experiment

Equation 7 was used in the calculations for the experiment. Where:

q is the heat input which was 100.8 Btu/hr-ft^2 for all samples

w is the heat capacity of the apparatus, 0.316 Btu/°F-ft^2.

R is the inside radius of the inner tube, 0.0443 ft.

$\partial T/\partial t$ and $T_s - T_c$ are given for each sample with the time-temperature graphs.

The results are given in Table 7.

2. Analytical calculations

All the samples were of fine grade sand packed in a bed with stagnant air; therefore equation 16 was used, and $\beta = 1$ assumed.

The thermal conductivity of the stagnant air, k_g, was selected as 0.0164 Btu/hr-°f for the mean temperature of 135°F.

k_s = 1.075 Btu/hr-ft°F

The results are given in Table 7.

TABLE 7

Comparison of experimental and analytical results

Sample No.	Sand size of Tyler Standard	Experimental Thermal conductivity in Btu/hr-ft-°F	Analytical thermal conductivity in Btu/hr-ft-°F
1	50 - 60	0.2152	0.2155
2	60 - 80	0.2266	0.2254
3	80 - 100	0.2427	0.2379
4	100 - 200	0.2132	0.2066
5	200>	0.2101	0.2455

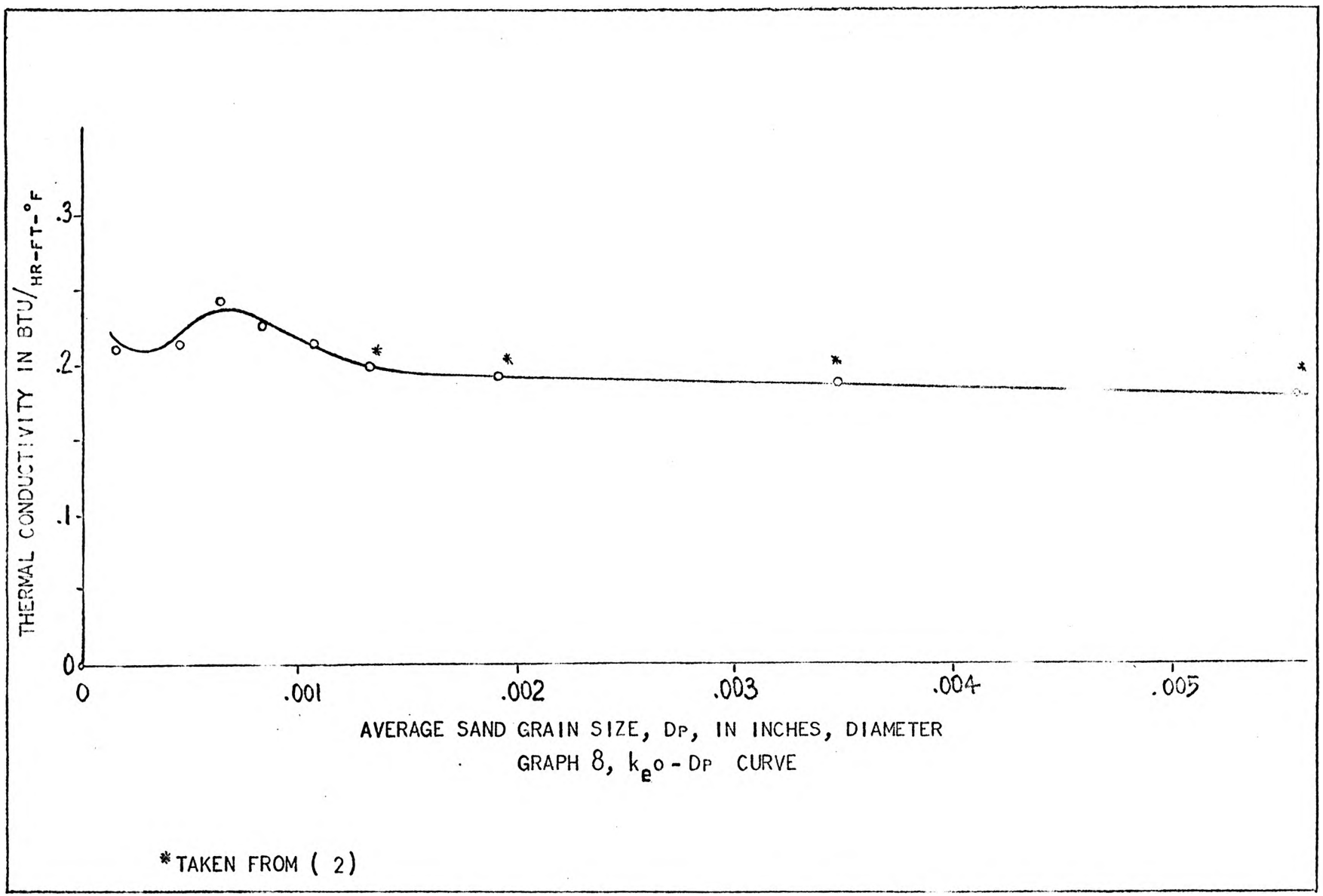

GRAPH 8, $k_{e}o$ - Dp CURVE

*TAKEN FROM (2)

VI. CONCLUSIONS

1. In the first three sand samples (50 −60, 60 − 80, 80 −100 particle sizes of Tyler Standard Screen Scale mesh), the analytical and experimental results were close to each other, and the ratios of the difference between the experimental and analytical results to the experimental thermal conductivities were 0.0014, 0.0053, and 0.0198, respectively. The thermal conductivities of the above samples increased as the granular size of sand decreased.

2. In the fourth sample (100 −200 of Tyler Standard Screen Scale mesh), the experiment showed that the analytical and experimental results were not as close to each other as were the first three samples. The ratio of the difference between the experimental and analytical results to the experimental thermal conductivity was 0.031. The thermal conductivity decreased for the fourth sample whereas it increased for the first three samples.

3. In the fifth sample (smaller than 200 of Tyler Standard Screen Scale mesh), the analytical and experimental results obtained were completely different. The analytical result was considerably higher than the experimental result, 0.2455 and 0.2101 Btu/hr-ft- F, respectively.

4. As can be seen from the experimental results of the fourth and fifth samples, the analytical method of Yagi and Kunii (3) cannot be applied for very fine particles.

5. The experiment showed that the temperature gradient, and the differences between the temperatures at the center and at the wall slightly decreased when the temperature of the system was increased. Therefore, the effective thermal conductivity was not actually a constant, but instead it increased with temperature. The results which were obtained in this thesis are valid for the temperature range of 80 - 150°F.

APPENDIX

APPENDIX

THE SOLUTION OF THE PARTIAL DIFFERENTIAL EQUATION FOR SYMMETRICAL RADIAL HEAT FLOW

The differential equation is

$$(\partial^2 T/\partial r^2) + (1/r)(\partial T/\partial r) = (1/K)(\partial T/\partial t) \quad . \quad . \quad . \quad . \quad . \quad (1)$$

using Laplace transform

$$L(u) = \bar{u} = \int_o^\infty e^{-\bar{u}t} f(t)dt$$

The Laplace transform of the equation is

$$(d^2\bar{u}/dr^2) + (1/r)(d\bar{u}/dr) = (1/K)(u\bar{u})$$

substituting $u/K = a^2$

$$(d^2\bar{u}/dr^2) + (1/r)(d\bar{u}/dr) - a^2\bar{u} = 0 \quad . \quad . \quad . \quad . \quad . \quad (17)$$

The solution by the zero-order Bessel equation is

$$\bar{u} = AI_o(ar) + BK_o(ar) \quad . \quad . \quad . \quad . \quad . \quad (18)$$

since $r = 0$

$$K_o = \infty$$

Then the solution is

$$\bar{u} = AI_o(ar) \quad . \quad . \quad . \quad . \quad . \quad (19)$$

For equation

$$q = k(\partial T/\partial r) + w(\partial T/\partial t) \quad . \quad . \quad . \quad . \quad . \quad (2)$$

using Laplace transform

$$k(d\bar{u}/dr) = (q/u) - wu\bar{u}$$

substituting value of $\bar{u}$

$$k[dAI_o(ar)/dr] = (q/u) = wuAI_o(ar)$$

$$A[kaI_1(ar) + wuI_o(ar)] = q/u$$

at $r = R$

$$A = (q/u)[kaI_1(aR) + wuI_o(aR)] \quad . \quad . \quad . \quad . \quad . \quad (20)$$

then

$$\bar{u} = q[I_o(ar)]/u[kaI_1(aR) + wu\, I_o(aR)] \quad \ldots\ldots (21)$$

by using the Inversion Theoren

$$T = \frac{q}{2\pi i} \int_{r-1}^{r+1} \frac{I_o(\mu r) e^{\lambda t} d\lambda}{\lambda[KaI_1(\mu R) + w\lambda I_o(\mu R)]} \quad \ldots\ldots (22)$$

where $\mu^2 = \lambda/K$.

The integrand of Equation (22) has a double pole at $\lambda = 0$ and single poles at the roots of

$$kaI_1(\mu R) + w\lambda I_o(\mu R) = 0 \quad \ldots\ldots (23)$$

Since I_o and I_1 in the Equation (23) are positive functions, it follows that all the roots are negative and consequently, the terms in T corresponding to these roots contain a negative exponential which tends to zero as t increases.

On expanding the various functions of the Equation (23) in power series, and taking the limit $\lambda \to 0$, it is found that the residue is

$$T = \frac{q}{2\pi i} \left[t + \frac{r^2}{4K} - \frac{R^2 (4Kw + kR)}{8K (2Kw + kR)} \right] / (w + kR/2K) \quad (24)$$

And by Cauchy residue theorem it follows that equation multiplied by $2\pi i$ is the term in T corresponding to $\lambda = 0$.

Thus,

$$T = \frac{q}{(w + kR/2K)} \left[t + \frac{r^2}{4K} - \frac{R^2 (4Kw + kR)}{8K (2Kw + kR)} \right] \quad (25)$$

BIBLIOGRAPHY

1. Thomas, T. S. E., "A Method of Measuring the Thermal Constants of Granular Materials," British Journal of Applied Physics, Vol. 8, 1957, pp. 403 - 405.

2. Patel, K. M., "The Effects of Granular Size on the Thermal Conductivity of Sand," M. S. Thesis, The University of Missouri, School of Mines and Metallurgy.

3. Yagi, Sakae and Kunii, Daizo, "Studies on Effective Thermal Conductivities in Packed Beds," A. I. Ch. E. Journal, Vol. 3, No. 3, 1957, pp. 373 - 381.

4. Saunders, O. A., "Simplitude and the Heat Flow through a Granulated Material," Philosophical Magazine and Journal of Science, Vol. 13, 1932, p. 1186.

5. Ranz, W. E., "Friction and Transfer Coefficients for Single Particles in Packed Beds," Chem. Eng. Progress, Vol. 48, No. 5, 1952, pp. 247 - 253.

6. Schumann, T. E. W. and Voss, V., "Heat Flow through Granulated Material," Fuel, Vol. 13, 1934, pp. 249 - 265.

7. Sivadasan, A. M., "Methods for Determination of the Thermal Conductivity of Solids," M. S. Thesis, The University of Missouri, School of Mines and Metallurgy, No. T1505, 1963, pp. 92 - 100.

8. Waddams, A. L., "Flow of Heat through Granular Materials," Chem. and Ind., Journal, Vol. 63, No. 23, 1944, pp. 206 - 210.

9. Weininger, J. L. and Schneider, W. C., "Thermal Conductivity of Granular Beds Filled with Compressed Gases," Ind. and Eng. Chem., Vol. 43, 1951, pp. 229 - 233.

VITA

The author, Fikri Yalvac, was born on September 18, 1933, in Erzurum, Turkey. After completing his grade and high school education in Erzurum, he was enrolled in the Engineering (Technical) School of Istanbul from 1952 to 1956, and he received his B. S. degree in Mechanical Engineering in June, 1956.

After his graduation, he worked as a Mechanical Engineer for the Ammunition Factory of Kirikkale, Turkey, from 1956 to 1957. He was assistant to the Professor of Thermodynamics in the Engineering School of Istanbul from 1957 to 1960 while holding a part time job in a manufacturing company in Istanbul. He was drafted in the very beginning of 1960, and served in the Turkish Army as an engineer lieutenant for one and a half years. After completing his military service, he worked for the British Petrol Company in Istanbul for six months. Then he came to the United States in January, 1962.

After having English courses in Queens College of New York, he entered the University of Missouri, School of Mines and Metallurgy, in February, 1963, for a Master of Science Degree in Mechanical Engineering.